Effects of Sahel Dust Layers upon Nocturnal Cooling of the Atmosphere (ECLATS Experiment)

DANIEL GUEDALIA, CLAUDE ESTOURNEL AND RAOUL VEHIL

Laboratoire d'Aérologie, 31062 Toulouse cedex, France

(Manuscript received 30 April 1983, in final form 29 September 1983)

ABSTRACT

A study of the effect of a desert aerosol layer on the nocturnal cooling of the atmosphere is presented. The experimental data were obtained during the ECLATS experiment which was run in the Sahel region of the Niger in November 1980. This study uses measurements of thermodynamic and radiative parameters, aerosol size distribution, and a radiative model. The results show that the presence of a dust layer at night increases the downward infrared flux at the surface (and then modifies the energy budget) and increases the radiative cooling rate of the atmosphere, slightly in the layers near the ground ($\sim$0.15 K h^{-1}) and in a more important way at the top of the haze layer.

1. Introduction

For several years, a growing interest has been shown in the modifications of the radiative budget of the atmosphere brought about by stratospheric or tropospheric aerosol layers and their short-term and long-term effects on the climate.

An important example is the case of dust layers from desert regions which can move over long distances. This is the case for dust originating over the deserts of Asia (Shaw, 1980; Duce *et al.*, 1980) and over the African deserts arriving at the American coast (Carlson and Prospero, 1972; Prospero and Carlson, 1972).

The particle size distribution and optical properties of these desert aerosols have been studied by several authors, e.g., the Saharan dust (Shütz and Jaenicke, 1974; Carlson and Caverly, 1977), the Negev desert dust (Levin and Lindberg, 1979) and the Asian desert dust (Darzi and Winchester, 1982). Numerical simulation has allowed the radiative heating or cooling rate to be calculated in these tropospheric aerosols layers (Harshvardhan and Cess, 1978; Carlson and Benjamin, 1980). Yet, however useful these simulations may be, very little validation has been carried out owing to the lack of *in situ* measurements of the radiative fluxes in the hazy atmospheres.

So, in November and December 1980, the ECLATS experiment was run in the Sahel region of the Niger. The purpose of this experiment was to study the influence of the radiative term on the evolution of the internal structure of the atmospheric boundary layer during both daytime and nighttime periods. A complete description of ECLATS will be found in Druilhet and Tinga (1982).

This paper presents only the results concerning the modification of nocturnal cooling of the atmosphere caused by the Sahel aerosol.

The experimental data presented here mainly concern the radiative fluxes in the haze layer obtained using a tethered balloon for the first few hundred meters and an aircraft measurement system for the levels above. We measured the vertical profiles of temperature and water vapor simultaneously, which allowed us to calculate the radiative cooling for a dust-free atmosphere. The aerosol particle size distribution was also measured by aircraft measurement. Finally, using the aerosol properties, a series of numerical simulations was carried out in order to interpret the direct measurements of radiative cooling. The interest in this study includes a comparison of the experimental data with the results of the numerical simulation of the radiative cooling rate in an aerosol layer.

2. Basic instrumentation

a. Tethered balloon

The main instrumentation used in the study of the nocturnal layer was a tethered balloon of volume 5 m^3 which allows a payload of 2.5 kg to be carried. It was used to measure three types of parameter:

1) Mean thermodynamic parameters: pressure, dry- and wet-bulb temperature, wind direction and wind speed.

2) The upward and downward infrared fluxes using two pyrgeometers one above and the other below the balloon. (The pyrgeometers weighed 460 g and were built in our laboratory.)

3) The horizontal components of the wind speed were measured using a hot wire anemometer.

All the data were sent to the ground by telemetry.

b. Ground measurement

The components of the energy balance at the surface, in particular the upward and downward IR fluxes, were measured using Eppley pyrgeometers.

c. Aircraft measurements

An aircraft type Hurel-Dubois 34 was used to measure thermodynamic, turbulent and radiative parameters as well as the particle size distribution.

3. Radiative model

a. Clear atmosphere

A description of the radiative model used for clear atmospheres can be found in Estournel *et al.* (1983). It is a high spectral resolution model (232 intervals between 4 and 100 μm), which uses the transmission functions of Moskalenko (1968, 1969) and Golubitskiy and Moskalenko (1968) between 4 and 22 μm and those of Goody (1964) between 22 and 100 μm. Spectral resolution is roughly 5 cm^{-1} in the atmospheric window, giving a good description of this important range for radiative exchanges.

The net monochromatic flux at level z was calculated using the expression

$$F(z) = [Bg - B(0)]T_{0z} + B(z^*)Tzz^* - \int_0^{z^*} Tzz' \frac{d}{dz} B(z')dz', \quad (1)$$

where Bg is Planck's function at the ground, $B(z)$ Planck's function at z level, z^* the level of the top of the model and Tz_1z_2 the transmission of the layer limited by levels z_1 and z_2, using the diffusivity factor approximation.

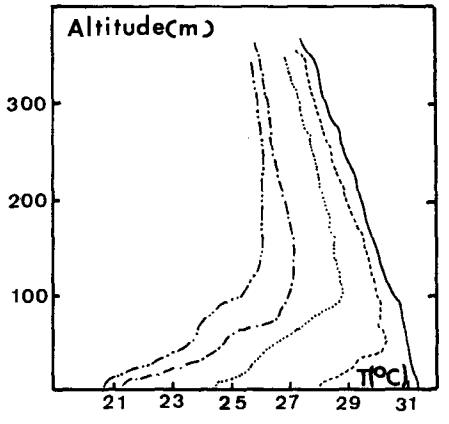

FIG. 1. Temperature profiles measured during the night of 27–28 November 1980: 1700 (solid line), 1840 (dashed line), 2150 (dotted line), 0140 (dot-dash line) and 0430 (double dot-dash line). All times local standard.

TABLE 1. Comparison between the IR fluxes at the surface measured during the night of 27–28 November and those calculated with the model for a clear atmosphere. The last column gives the total number of particles (cm^{-2}) in the haze layer.

Time (LS)	Measured flux ($W\ m^{-2}$)	Calculated flux ($W\ m^{-2}$)	Percent increase	Number of particles
2155	373	340	9.7	3.26×10^8
0140	360	332	8.4	2.84×10^8
0433	352	327	7.7	1.65×10^8

b. Aerosol contribution

The delta Eddington method was used in the atmospheric window (7.5–13 μm) to compute the radiative fluxes in the hazy atmosphere. The scattering and extinction efficiency factors, as well as the asymmetry factor, were calculated using Mie theory. For the optical depth of the aerosol layer and also for the small values of the asymmetry factor and the simple scattering albedo of the particle distributions used in this study, Wiscombe and Joseph (1977) show that the approximation errors are of order 1%. Moreover, the results of this study have little dependence on the sophistication of the scattering computation, since this process contributes slightly to the values of the infrared fluxes.

4. Experimental results

The results presented here were obtained during the night of 27–28 November 1980, during which the dust concentration was high (visibility about 3 km). The depth of the haze layer, determined by aircraft, remained at 1200 m during the night. Fig. 1 shows the temperature profiles measured with the balloon from 1700 to 0430 (all times local standard); a nocturnal inversion layer growing near the ground can be seen below 100 m; an important cooling was also observed in the layers above the nocturnal inversion.

a. Downward infrared fluxes

Table 1 shows the values of the IR fluxes measured at the surface, those calculated for a clear atmosphere and the total number of particles contained in the haze layer calculated from distribution 1 of Fig. 4 at three times during the night.

Thus, a homogeneous layer of aerosol at night provides an increase in the value of the downward IR flux of 25–35 Wm^{-2}; this increase, which is dependent on the dust concentration, modifies the energy budget at the surface level leading to a decrease of surface cooling.

The increase in IR flux is also observed from the measurement, made at constant levels, by the aircraft between 0600 and 0630 (Fig. 2). The value at 1500 m, i.e., above the haze layer, was close to that calculated by the dust-free model; on the other hand, the IR fluxes measured at 55 and 290 m in the haze layer, exceeded those calculated for a dust-free atmosphere by 22 and 17 W m^{-2}, respectively.

b. Radiative cooling rate of the atmosphere

The radiative cooling rate in the haze layer was obtained from the net flux measured with the two pyrgeometers mounted on the tethered balloon. The flux value is calculated from the formula given by Albrecht and Cox (1977):

$$L = \epsilon_0 \sigma T_s^4 - kV + \beta\sigma(T_s^4 - T_d^4), \qquad (2)$$

where L is the atmospheric IR flux, ϵ_0 the emissivity of the thermopile surface, σ Boltzman's constant, T_s and T_d the temperatures of the cold junctions and the hemisphere respectively, V the output voltage and k and β calibration constants. The two pyrgeometers mounted on the balloon and the ground-based Eppley were simultaneously calibrated using a blackbody. The determination of the β coefficient in Eq. (2) was not very accurate; therefore, measurements presenting an important temperature difference between the cold junctions and the hemisphere of the pyrgeometer were eliminated. This is the case with measurements taken in the inversion layer where a thermic lack of balance exists in the different parts of the pyrgeometer during the continuous ascent of the balloon. The experimental data of the net flux were fitted to calculate the radiative cooling rate; the horizontal lines in the figures represent the range of uncertainty of the slope of the net flux between two levels.

The measured radiative cooling rates and those calculated with the dust-free model are presented in Fig. 3. The presence of an aerosol layer enhances slightly the radiative cooling rate of the atmosphere at night. In the present case, the cooling rate due to the aerosol is about 0.05 K h^{-1} for a total measured cooling rate between 0.1 and 0.3 K h^{-1}.

c. Particle size distribution of Sahel aerosols

On board the aircraft, two optical counters were used: an FFSP-type Knollenberg (for particle radii between 0.25 and 3.75 μm) and a Kratel model Partoscope A (between 0.225 and 1.5 μm). Particle size distribution was also calculated by Fouquart *et al.* (1983) by King's (1978) inversion method, using the optical thickness measured at nine wavelengths in the visible and near-infrared spectrum. Fig. 4 shows the size distribution measured by aircraft counters at the beginning of the night (~1800) as well as the size distribution calculated by the inversion method. It can be seen from the figure that the Knollenberg and Kratel counters underestimate the number of particles of ra-

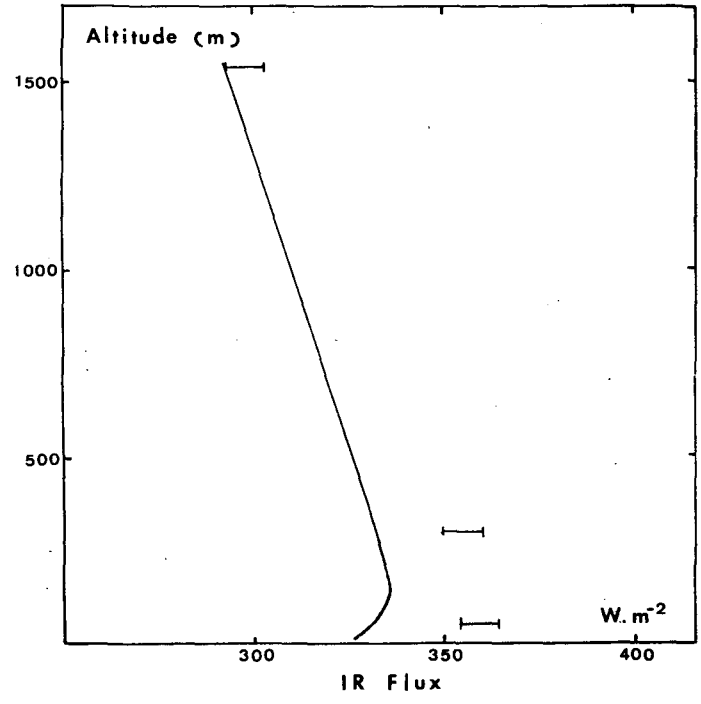

FIG. 2. Downward IR flux between 0600 and 0630 on 28 November 1980. Aircraft measurements (horizontal line); computed values by dust-free atmosphere model (solid line).

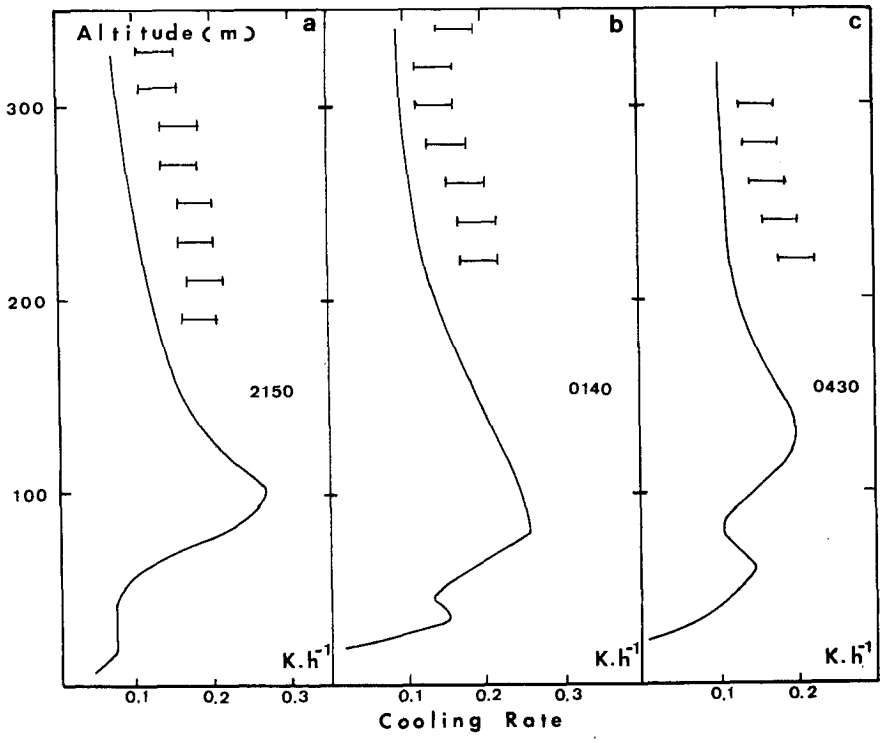

FIG. 3. Radiative cooling rate in the nocturnal boundary layer, computed by dust-free atmosphere model at different times: (a) 2150, (b) 0140, (c) 0430. Measured values (horizontal line).

dius < 1 μm; the Knollenberg counter, however, gave results in quite good agreement with the calculated distribution for large particles.

Figure 5 shows the particle size distribution measured with the Knollenberg and Kratel counters at various altitudes on the night of 27–28 November. It can be seen that the particle size distribution is practically constant throughout the haze layer.

5. Numerical simulation of the radiative effect of the aerosol

The complex index of refraction of aerosols used in our infrared model was that determined by Volz (1973) for Saharan dust. Two particle size distributions were used: that determined by the inversion method, No. 1, and that corresponding to the addition of the data obtained with the Kratel ($r < 1.5$ μm) and with the Knollenberg ($r > 1.5$ μm) counters, No. 2.

a. Simulations for the night of 27–28 November 1980

A numerical simulation was carried out with the size distributions No. 1 and No. 2 at three different times during the night of 27–28 November 1980. The aerosol concentration used in the model was calculated taking into account the data of a ground-based integrating nephelometer. Table 2 shows the measured and calculated values of downward IR flux at ground level.

It can be seen that the IR flux values calculated with the No. 1 distribution are very close to those measured at three moments during the night. However, the values calculated with the No. 2 distribution are lower than the measured values by approximately 10 W m^{-2}. It can be seen from Fig. 6 that the radiative cooling rate calculated with either of the distributions are in close agreement with the measured values. The difference of cooling rate calculated with each of the two distributions is small, because the largest difference between them appears in the number of small particles (radius < 1 μm); these small particles have only a limited influence on the divergence of the radiative IR flux. For the simulation made with the two distributions, the difference between the calculated cooling rates remains lower than 0.02 K h^{-1}.

b. Simulation on the limits of the aerosol effects during the nighttime

We carried out a series of simulations to show the effect of the Sahel aerosol at night when the particle concentration is increased. The particle size distribution used in the model was No. 1, i.e., that determined from the inversion of optical thicknesses (Fouquart *et al.*, 1983, 1984). The aerosol concentration used in the model was represented by its total optical thickness. Therefore, a 1200 m deep haze layer containing the size distribution represented in Fig. 4, provides a total optical thickness of 0.45 for $\lambda = 10$ μm (corresponding to 1.7 for $\lambda = 0.5$ μm).

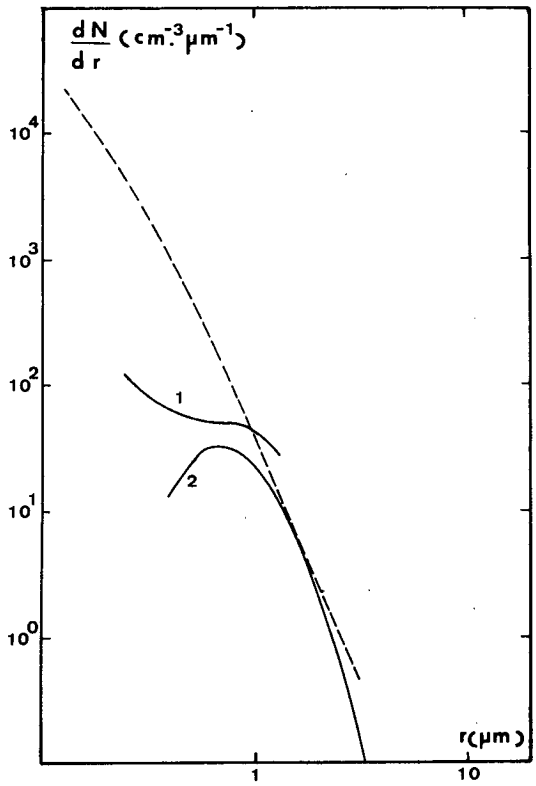

FIG. 4. Size distribution (solid lines) of Sahel aerosols measured by (1) Kratel counter, (2) Knollenberg counter. Dashed line shows that computed by inversion method.

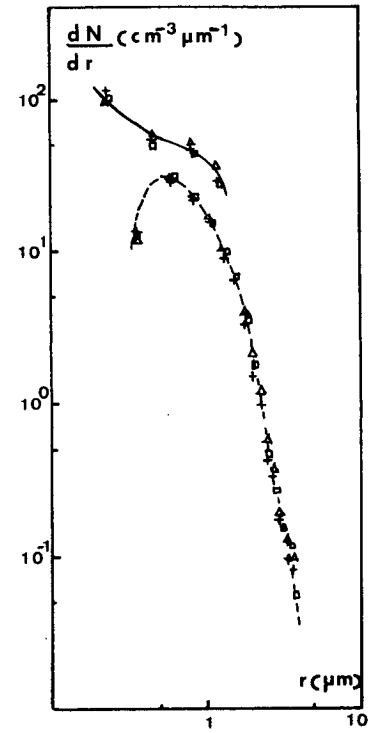

FIG. 5. Aerosol size distribution measured by Kratel (solid line) and Knollenberg (dashed line) at several altitudes in the haze layer: squares, 150 m; plus signs, 220 m; and triangles, 830 m.

A series of simulations was made from the temperature profile of 2155 for optical thickness values for the haze layer between 0.45 and 2.7. Fig. 7 shows the radiative cooling rate due to the aerosols only, i.e., the total cooling from which the dust-free value has been subtracted, henceforth called *relative* cooling. The greatest relative cooling occurs at the top of the haze layer; at top level, the cooling increases with the optical thickness ($\sim$0.4 K h^{-1} for $\tau_{10} = 2.7$). A similar result was obtained by Carlson and Benjamin (1980) with Saharan aerosol simulations. On the other hand, in the first few hundred meters, radiative cooling reaches a limit value even though the optical thickness increases. In the first 100 m, one can even see a decrease in radiative cooling as τ increases. But at the same time, the IR flux at the surface increases with the optical thickness; this excess is 91 W m^{-2} for $\tau_{10} = 2.7$ with respect to dust-free atmosphere.

Thus, in the event of a very dense haze layer, the strong cooling at the top and the diminution of cooling at the surface will give rise to vertical instability of the nocturnal layer.

6. Conclusion

One of the objectives of the ECLATS experiment was to study the nocturnal boundary layer in the presence of a dry haze layer. This paper presents the results concerning the modification of natural nocturnal cooling caused by the Sahel aerosol.

The main interest of this study lies in the experimental data obtained for radiative cooling and for aerosol size distribution.

It was shown that the presence of an aerosol layer at night increases the downward IR flux at the surface and the radiative cooling rate of the atmosphere. The experimental data and the numerical simulation also allowed the limits of aerosol action to be defined during the night:

- The downward IR flux at the surface increases with the aerosols concentration, e.g., for an optical thickness (at 10 μm) of 2.7, the increase is 91 W m^{-2} with respect to a dust-free atmosphere.

TABLE 2. Downward IR fluxes measured on the night of 27–28 November 1980 and calculated from the model.

Local time	Measured value (W m^{-2})	Calculated value: Distribution 1	Calculated value: Distribution 2	Calculated value: Dust-free atmosphere
2155	373	376	365	340
0140	360	362	348	332
0430	352	348	337	327

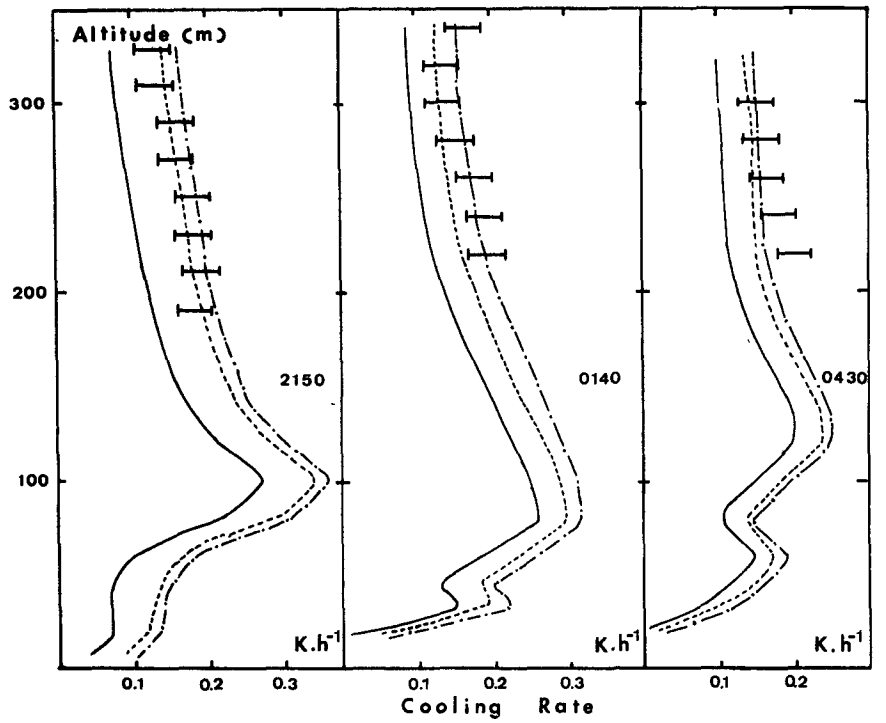

FIG. 6. Radiative cooling rate computed by model: dust-free atmosphere (solid line); with aerosol size distribution No. 2 (dashed line); No. 1 (dot-dash line). Measured values (horizontal line).

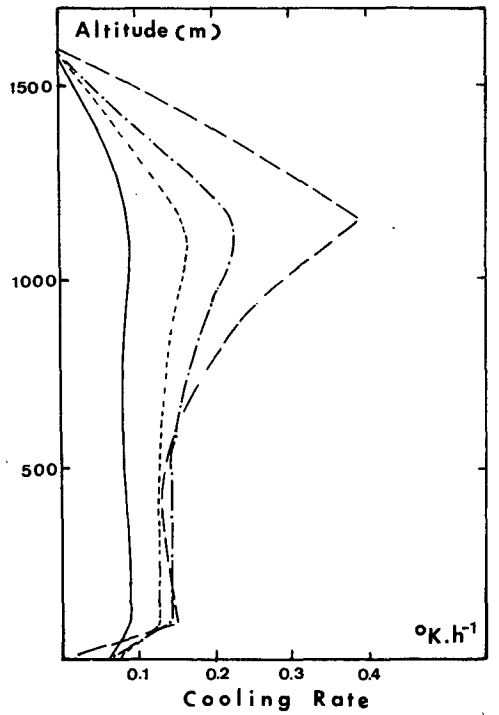

FIG. 7. Relative radiative cooling rate (see text) in a haze layer for different optical thicknesses, calculated by model. For: $\tau_{10} = 0.45$ (solid line), $\tau_{10} = 0.9$ (dotted line), $\tau_{10} = 1.35$ (dot-dash line) and $\tau_{10} = 2.7$ (dashed line).

- The radiative cooling rate is important at the top of the haze layer and increases as the amount of aerosol increases.
- However, the radiative cooling rate in the first few hundred meters reaches a limiting value and even decreases as the dust concentration increases.

The radiative effects occurring at the top and at the base of the haze layer could give rise to vertical instability in the atmospheric nocturnal layer when the haze is very dense.

Acknowledgments. The authors wish to thank A. Druilhet, chief-investigator of ECLATS, and J. Fontan who has been the encourager of the ECLATS project.

We also thank, P. Durand and A. Herrada for their compilation of aircraft data, J. C. Medale for his participation in the experimental phase, Y. Fouquart and A. Cerf for helpful discussions on radiation problems, and A. Lopez for his suggestions on aerosol data. We are grateful to the University of Niamey and especially to M. Tinga for their assistance. This research was supported by the A. T. P. "Recherches Atmosphériques" of Institut National d'Astronomie et Géophysique.

REFERENCES

Albrecht, B., and S. K. Cox, 1977: Procedures for improving pyrgeometer performance. *J. Appl. Meteor.*, **16**, 188–197.

Carlson, T. N., and J. M. Prospero, 1972: The large scale movement of Saharan air outbreaks over the northern equatorial Atlantic. *J. Appl. Meteor.*, **11**, 283–297.

——, and R. S. Caverly, 1977: Radiative characteristics of Saharan dust at solar wavelengths. *J. Geophys. Res.*, **82**, 3141–3152.

——, and S. G. Benjamin, 1980: Radiative heating rates for Saharan dust. *J. Atmos. Sci.*, **37**, 193–213.

Darzi, M., and J. W. Winchester, 1982: Resolution of basaltic and continental aerosol components during spring and summer within the boundary layer of Hawai. *J. Geophys. Res.*, **87**, 7262–7272.

Druilhet, A., and A. Tinga, 1982: Présentation de L'expérience ECLATS. *La. Météorologie*, 29–30, 203–211.

Duce, R. A., C. K. Unni, B. J. Ray, J. M. Prospero and J. T. Merrill, 1980: Long-range atmospheric transport of soil dust from Asia to the tropical north Pacific; temporal variability. *Science*, **209**, 1522–1524.

Estournel, C., R. Vehil, D. Guedalia, J. Fontan, and A. Druilhet, 1983: Observations and modeling of downward radiative fluxes (solar and infrared) in urban/rural areas. *J. Climate Appl. Meteor.*, **22**, 134–142.

Fouquart, Y., B. Bonnel, G. Brogniez, A. Cerf, M. Chaoui, L. Smith and J. C. Vanhoutte, 1983: Size distribution and optical properties of Saharan aerosols during ECLATS. *Workshop of Climatic Effects of Aerosols.* Williamsburg, W.M.O.-I.R.C.

——, ——, ——, ——, ——, ——, ——, ——, ——, and ——, 1984: Size distribution and optical properties of saharan aerosols during ECLATS. *Aerosols and their Climatic Effects* (in press).

Golubitskiy, B. M., and N. I. Moskalenko, 1968: Spectral transmission functions in the H_2O and CO_2 bands. *Atmos. Oceanic Phys.*, **4**, 194–203.

Goody, R. M., 1964: *Atmospheric Radiation.* Oxford University Press, 436 pp.

Harshvardhan, and R. D. Cess, 1978: Effect of tropospheric aerosols upon atmospheric infrared cooling rates. *J. Quant. Spectrosc. Radiat. Transfer*, **19**, 621–632.

King, M. D., 1978: Aerosol size distributions obtained by inversion of spectral optical depth measurements. *J. Atmos. Sci.*, **35**, 2155–2167.

Levin, Z., and J. D. Lindberg, 1979: Size distribution, chemical composition, and optical properties of urban and desert aerosols in Israël. *J. Geophys. Res.*, **84**, 6941–6950.

Moskalenko, N. I., 1968: The spectral transmission function in some water-vapor bands and in the CO and CH_4 bands in the infrared. *Atmos. Oceanic Phys.*, **4**, 443–446.

——, 1969: The spectral transmission function in the bands of the water-vapor, O_3, N_2O, and N_2 atmospheric components. *Atmos. Oceanic Phys.*, **5**, 678–685.

Prospero, J. M., and T. N. Carlson, 1972: Vertical and areal distribution of Saharan dust over the western equatorial North Atlantic Ocean. *J. Geophys. Res.*, **77**, 5255–5265.

Schütz, L., and R. Jaenicke, 1974: Particle number and mass distributions above 10^{-4} cm radius in sand and aerosol of the Sahara desert., *J. Appl. Meteor.*, **13**, 863–870.

Shaw, G. E., 1980: Transport of Asian desert aerosol to the Hawaiian Islands. *J. Appl. Meteor.*, **19**, 1254–1259.

Volz, F., 1973: Infrared optical constants of ammonium sulfate, Sahara dust, volcanic pumice and fly ash. *Appl. Opt.*, **12**, 564–568.

Wiscombe, W. J., and J. H. Joseph, 1977: The range of validity of the Eddington approximation. *Icarus*, **32**, 362–377.